Available online at www.sciencedirect.com
ScienceDirect
Physica B 385–386 (2006) 1315–1317
PHYSICA B
www.elsevier.com/locate/physb

Neutron optical imaging study of neutron moderator and beam extraction system

J. Füzi[a,b,*], E. Dávid[c], T. Kozlowski[d], P. Lewis[d], G. Messing[c], F. Mezei[d,e], S. Penttila[d], L. Rosta[a], M. Russina[e], Gy. Török[a]

[a] *Research Institute for Solid State Physics and Optics, H-1525 Budapest, Hungary*
[b] *Transilvania University, R-2200 Brasov, Romania*
[c] *OPEN Optoelectronics, 1121 Budapest,Hungary*
[d] *Los Alamos National Laboratory, Los Alamos, NM 87545, USA*
[e] *Hahn-Meitner-Institut, 14109 Berlin, Germany*

Abstract

The study of the performance of a cold-hydrogen moderator and a supermirror-based neutron beam extraction system of the flight path 12 at LANSCE has been performed based on energy-resolved neutron optical imaging. We have developed a pinhole camera system with a 2D position-sensitive ^{3}He multiwire proportional chamber neutron detector with delay line position encoding (0.75 mm pixel size), together with a standalone time-of-flight electronic system with 1.2 μs dead time. We have determined the efficiency, resolution, and counting rate saturation of the detector. In particular, we have considered an impact of these parameters on the quality of the images. The neutron images of the moderator were taken as a function of the neutron wavelength given by the time-of-flight information. The images were recorded as arrays of $256 \times 256 \times 2000$ pixels; x and y coordinates, and time of flight. Information obtained from the images includes a distribution of the brightness on the neutron moderator, the efficiency and geometrical accuracy of the beam extraction system, and the reflectivity of the supermirror-coated elements of its optics. Our results demonstrate that the pinhole optical camera-based neutron imaging method combined with time-of-flight information is an extremely efficient tool to characterize neutron sources and neutron beam extraction systems.

PACS: 29.27.Eg; 03.75.Be; 29.25.Dz

Keywords: Neutron imaging; Spallation sources; Neutron optics

1. Introduction

A fast and reliable measurement method has been sought for surveying the condition of a neutron beam extraction system and for determining the characteristics of a neutron moderator which typically are available as results of computer modeling [1]. We have developed a neutron imaging technique based on a pinhole camera and a 2D position-sensitive delay-line encoded multiwire ^{3}He ion chamber detector. We have tested the device by measuring the brightness of the flight path 12 (FP12) unique partially coupled cold-hydrogen moderator operated in back-scattering and flux-trapped geometry at the Los Alamos Neutron Scattering Center (LANSCE) [2]. Also we have taken images of the FP12 neutron guide system to study its performance—alignment accuracy and average reflectivity of the supermirror plates. The results allow the evaluation of the wavelength-dependent guide transfer function.

2. Experimental setup

Fig. 1 shows the setup of the experiment, dimensions are in mm, the vertical-to-horizontal scale is 50:1, M is the moderator surface, E the FP12 neutron beam extraction guide system [1], including a shutter section, D the

---

[*] Corresponding author. Tel.: +36 1 392 2222 1738; fax: +36 1 392 2501.
E-mail address: fuzi@szfki.hu (J. Füzi).

0921-4526/$ - see front matter © 2006 Elsevier B.V. All rights reserved.
doi:10.1016/j.physb.2006.06.062

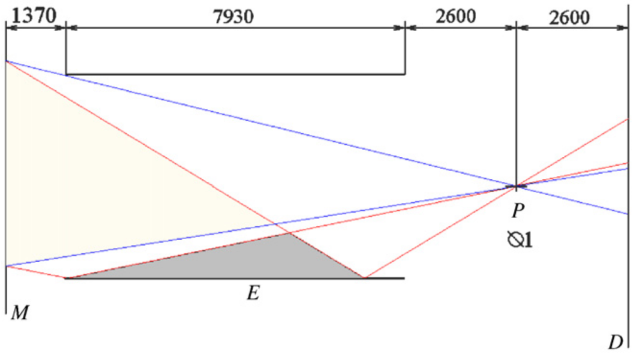

Fig. 1. Experimental setup on the FP12 at LANSCE.

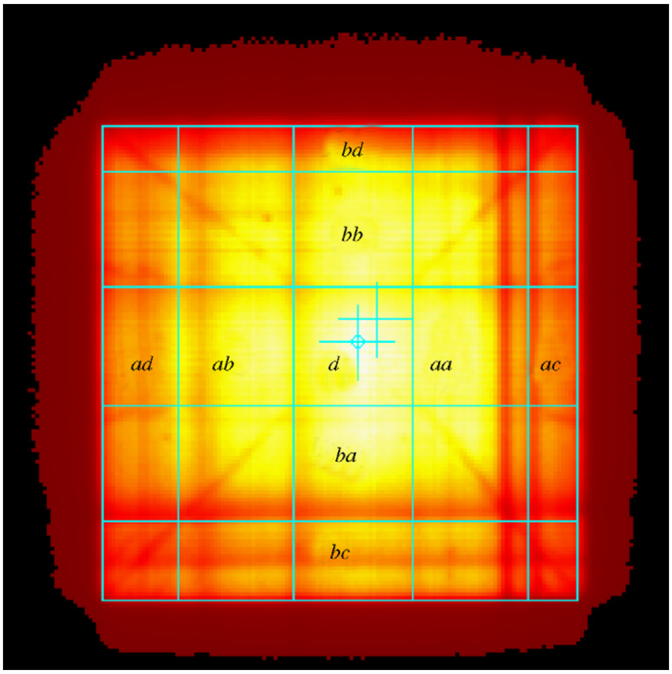

Fig. 2. Neutron image in the range 2.74–9.55 Å. Area d is direct view of the moderator, in areas aa, ab, bb, and ba the neutrons had one reflection, and in areas ac, ad, bc, and bd the neutrons had two reflections. The outer frame size is 142 × 142 pixels.

position-sensitive neutron detector, P is a 1 mm diameter pinhole in a *Cd* plate mounted on a boron-loaded polyethylene plate with a 25 mm hole. Also shown are the limits of the upper single reflection bb and the corresponding direct view region d for the neutron guide reflectivity estimation. It turned out that there was an eccentricity of 3.5 mm in horizontal and 4.5 mm in vertical direction of the pinhole with respect to the neutron guide axis. The neutron guide inner cross-sectional area is $9.5 \times 9.5\,\text{cm}^2$.

Fig. 2 shows our typical pinhole camera neutron image, together with the frames delimiting the direct view, single and multiple-reflection regions. The images were taken as a function of neutron time of flight [3], triggered by the incident proton pulse on the spallation target allowing the representation of measured quantities as a function of the accurate neutron wavelength Fig. 3.

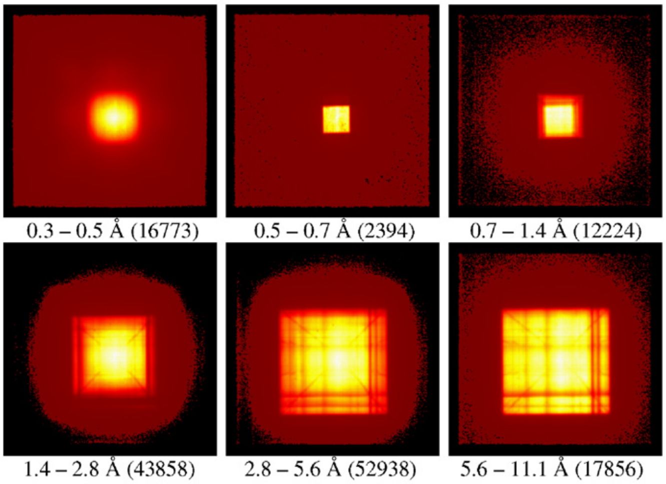
0.3 – 0.5 Å (16773) 0.5 – 0.7 Å (2394) 0.7 – 1.4 Å (12224)
1.4 – 2.8 Å (43858) 2.8 – 5.6 Å (52938) 5.6 – 11.1 Å (17856)

Fig. 3. Images of the non-attenuated beam in several wavelength ranges; the number of counts in the brightest pixels are shown in brackets; measurement time: 6662 s (133240 pulses).

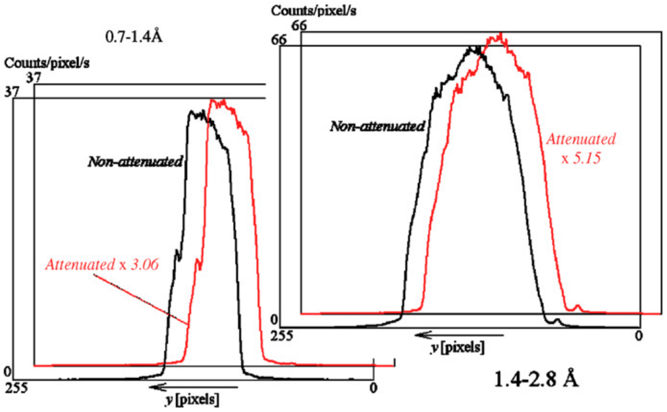

Fig. 4. Vertical cuts of the pinhole images indicating the proportionality between the saturated and non-saturated images.

3. Position-sensitive ^{3}He ion chamber neutron detector

The neutron images were recorded using a 2D position-sensitive delay-line encoded multiwire ^{3}He ion chamber detector with active area of $20 \times 20\,\text{cm}^2$, containing $p = 2.5$ bar ^{3}He gas, with an active thickness of $x = 3.5$ cm. The effective gas absorption is

$$\eta = 1 - \exp\left(-\frac{x}{\mu}\right) = 1 - \exp\left(-\frac{xp}{k}\lambda\right), \qquad (1)$$

where $k = 12.98$ cm bar Å. We measured two pinhole images in order to determine the detector saturation, one with non-attenuated beam and one through a polyethylene attenuator.

Even under heavily saturated conditions, the detector image is fairly proportional to the one taken in the non-saturated conditions. This is indicated in Fig. 4 where vertical cuts are plotted through the non-attenuated and attenuated beam images with different magnitude scales. This shows that the image remains proportional even when

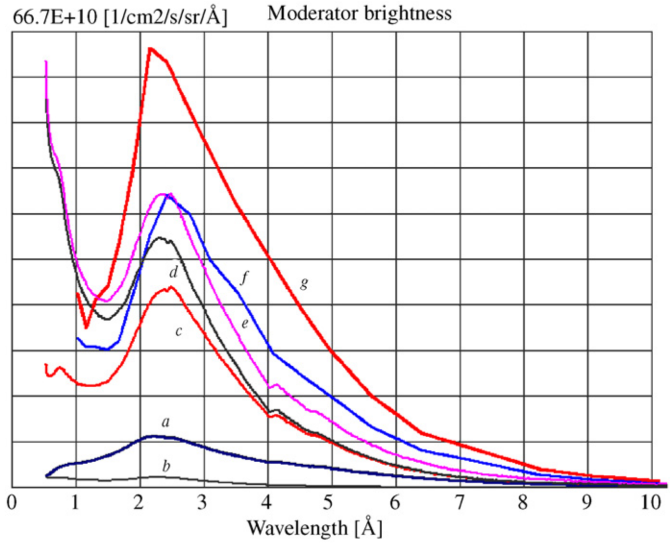

Fig. 5. Measured neutron spectra on the surface of the FP12 moderator as a function of the neutron wavelength, a: as measured, non-attenuated, uncorrected spectrum; b: as measured, attenuated, uncorrected spectrum; c: attenuated beam, PE attenuation correction; d: c with gas detection efficiency correction; e: d with air attenuation correction; f: results of scintillation detector measurement [1]; g: results of MC simulation [1].

the global count rate exceeds the saturation limit determined by the finite delay line length and the electronic processing performance.

4. Evaluation of FP12 moderator brightness

The measure of the performance of the neutron source is its moderator brightness. The neutron flux out from the moderator surface is given by

$$\Phi_{\mathrm{d}} = \frac{I}{\eta\, \mathrm{d}\lambda\, \mathrm{d}\Omega\, \mathrm{d}A\, t}, \tag{2}$$

where η is the detector neutron absorption efficiency given by Eq. (1), I the number of events measured on $n_x \times n_y$ pixels in one time bin, dA in cm^2 is the area of the pinhole (0.1 cm diameter pinhole at $l_{\mathrm{d}} = 2590$ mm from the detector), $t = n_{\mathrm{t}}\,0.05$ s is the effective measurement time (n_{t} is the number of counted neutron source pulses), $\mathrm{d}\lambda = 3956\,\tau/l_{\mathrm{m}}$ in Å is the elemental wavelength ($\tau = 0.051$ ms is the length of a time bin and l_{m} is the moderator–detector distance = flight length), and $\mathrm{d}\Omega = n_x n_y d^2/l_{\mathrm{d}}^2$ is the solid angle corresponding to the observed area where $d = 0.754$ mm is the pixel size. Substituting in Eq. (2), we obtain

$$\Phi_{\mathrm{d}} = \frac{l_{\mathrm{m}} l_{\mathrm{d}}^2 f}{\eta\, 3956\, \tau d^2\, dA} \frac{I}{n_x n_y n_t} \left[\frac{n}{\mathrm{cm^2\, s\, sr\, \AA}}\right]. \tag{3}$$

The measured direct neutron spectra on the moderator surface are plotted in Fig. 5 as a function of wavelength.

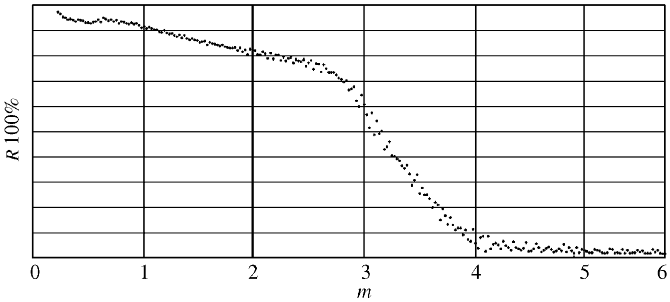

Fig. 6. Averaged reflectivity of the neutron guide mirror plates.

5. FP12 neutron guide assessment

The reflectivity of the supermirror plates of the neutron guides of the beam extraction system can be determined by computing the ratio between the number of detected neutrons in pixels corresponding to the reflected and direct neutrons, respectively (see Figs. 1 and 2). The reflectivity of the mirror plates averaged over the single reflection regions is plotted in Fig. 6 as a function of $m = \theta_{\mathrm{c}}/\theta_{\mathrm{c}}(^{\mathrm{nat.}}\mathrm{Ni})$. In reality, the reflectivity of a single mirror plate is better than that shown by these results since we are averaging several plates and also the alignment of the plates is not perfect. Dark stripes in the image of Fig. 2 are due to the imperfect alignment of the FP12 shutter section, which reduces the average reflectivity.

6. Conclusion

The pinhole optical camera and 2D position-sensitive neutron detector-based imaging system combined with time-of-flight information is proved to be an extremely efficient tool to study the variation of the neutron brightness on the moderator surface as well as the efficiency and geometrical accuracy of the beam extraction system and the determination of the reflectivity of the supermirror-coated elements of the beam extraction optics. With a single short exposure time image we can have a complete moderator and guide information as a function of neutron wavelength.

References

[1] P.-N. Seo, J.D. Bowman, M. Gericke, G. Greene, J. Long, G.S. Mitchell, S.I. Penttila, W.S. Wilburn, Nucl. Instr. and Meth. A 517 (2004) 285.

[2] G.J. Russell, et al. in: Proceedings of the 16th Meeting of the International Collaboration on Advanced Neutron Sources, Dusseldorf-Neuss, Germany, 2003, 833.

[3] OPEN Optoelectronics: OTDC-TOF—four channel time-to-digital converter for 2D time-of-flight measurements, ⟨www.openopto.kfkipark.hu/products/ODES⟩.